

Radio Science

RESEARCH ARTICLE

10.1029/2019RS006800

Key Points:

- Ionospheric E layer zonal electric field can be estimated using Ohm's law, conductivity model, and equatorial magnetometers observations
- A simplified vertical drift velocity model based on Ampere's and Ohm's laws is developed
- The performance of the new technique is better than IRI2016 and Anderson models in describing the C/NOFS vertical drift velocity observation

Correspondence to:

H. Marew,
hmarew@gmail.com

Citation:

Marew, H., Nigussie, M., Hui, D., & Damitie, B. (2019). A method of estimating equatorial plasma vertical drift velocity and its evaluation using C/NOFS observations. *Radio Science*, 54, 590–601. <https://doi.org/10.1029/2019RS006800>


Received 18 JAN 2019

Accepted 22 JUN 2019

Accepted article online 3 JUL 2019

Published online 19 JUL 2019

A Method of Estimating Equatorial Plasma Vertical Drift Velocity and Its Evaluation Using C/NOFS Observations

H. Marew^{1,2}, M. Nigussie¹, D. Hui³ , and B. Damitie¹

¹Washera Geospace and Radar Science Laboratory, Bahir Dar University, Bahir Dar, Ethiopia, ²Department of Physics, Debre Tabor University, Debre Tabor, Ethiopia, ³Indian Institute of Geomagnetism, Bombay, India

Abstract To understand the dynamics of the equatorial ionosphere and mitigate its effect on radio wave propagation, vertical ion drift velocity empirical models have been developed using limited ground-based and/or space-based observations. These models, however, have not yet been validated in detail using recent observations for sufficiently different longitudinal sectors. In this paper we have evaluated the performance of two empirical models and also propose a simplified vertical drift velocity model based on basic physics laws (i.e., Ampere's and Ohm's laws) that we call it parameterized drift velocity (PDV) model. These models have been applied to estimate the E region electric field and the associated F region $\mathbf{E} \times \mathbf{B}$ drift velocity using observed horizontal magnetic fields, due to equatorial electrojet current, as model driver input. Drift velocities obtained from these models are compared with the Communication/Navigation Outage Forecasting System (C/NOFS) satellite in situ vertical drift observations for different longitudinal sectors. It is found, for all longitudinal sectors considered in this study, that the vertical drift velocity obtained from a model based on physics laws has shown better agreement with C/NOFS observations as compared to the outputs of other empirical models. Moreover, it is shown that the Anderson empirical model performs better than the International Reference Ionosphere model.

1. Introduction

Equatorial ionosphere exhibits many interesting and unique plasma processes. Horizontally oriented geomagnetic field together with daytime eastward equatorial electric field (EEF), which is generated due to E region ionospheric dynamo (Farley et al., 1986; Haerendel & Eccles, 1992; Heelis, 2004), makes the equatorial ionosphere unique. The daytime eastward electric field drives intense current in the E region known as equatorial electrojet (EEJ) and produces plasma vertical drift $\mathbf{E} \times \mathbf{B}$ in the F region (Fejer & Kelley, 1980; Hui & Fejer, 2015; Kelley, 2009; Kelley et al., 2009; Sreeja et al., 2009). Moreover, it is also responsible for the equatorial ionization anomaly (EIA) and creates conducive conditions for equatorial spread-F (ESF) by driving the plasma to higher altitude particularly during the evening time (Sreeja et al., 2009). The EIA and ESF are exemplary equatorial ionospheric phenomena, which are known to disrupt the transionospheric propagating radio wave-dependent technologies such as communication, navigation, positioning, and surveillance (Sreeja et al., 2009). On the other hand, when the zonal electric field alters direction to the west, the plasma drifts downward and hence it can quench the development of ESF and EIA (Sridharan et al., 2009). The westward E field reverses the EEJ to the west when it is a counter electrojet.

Ionospheric E field and the associated plasma drift velocity models have been developed to understand in detail about the electrodynamics of the equatorial ionosphere (Anderson et al., 2004; Alken & Maus, 2009; Hysell & Burcham, 2000; Scherliess & Fejer, 1999). Alken and Maus (2009) used CHAMP satellite-derived latitudinal current profiles of the daytime EEJ in order to estimate the eastward electric field at all longitudes, seasons, and dayside local times. The model has been constructed from a data set of over 32,000 EEF estimates based on 6 years of CHAMP data during the years 2000 through 2006, and their model results agree well with Jicamarca Unattended Long-term Investigations of the Ionosphere and Atmosphere coherent scatter radar measurements. Hysell and Burcham (2000) also estimated the zonal ionospheric electric field using Jicamarca Unattended Long-term Investigations of the Ionosphere and Atmosphere radar observations of the EEJ at Jicamarca, and the results obtained are comparable to seasonally averaged incoherent scatter radar measurements.

Similarly, Scherliess and Fejer (1999) have developed an empirical climatological model for the quiet time F region equatorial vertical drift velocity using data from incoherent scatter radar observations at Jicamarca and ion drift meter on board the low-inclination Atmospheric Explorer E (AE-E) satellite from 1968 to 1992. The model has been developed by simultaneously fitting all satellite and radar vertical drift observations to a spherical harmonic function. The model gives F region vertical plasma drifts as a function of longitude, local time, season, and solar flux, and it describes the diurnal and seasonal variations of the equatorial vertical drift velocity for all longitudes and solar flux values. This model is included to the International Reference Ionosphere (IRI) model of the electron density to estimate the vertical drift velocity. In this work, the model is designated as IRI drift velocity model. The performance of this model has been tested against independent observations taken from different longitudinal sectors such as Brazilian, Indian, and Pacific regions, and it is found a good agreement between the observation and the model (Scherliess & Fejer, 1999). However, its performance has not been evaluated for wide longitudinal sector. The uncertainty of this model during moderate solar conditions is estimated to be about 6–7 m/s (Scherliess & Fejer, 1999).

Moreover, models used to describe the relationship between vertical drift velocity and the magnetic field from EEJ have been developed (Anderson et al., 2002, 2004; Anderson et al., 2006; Rastogi & Klobuchar, 1990). Anderson et al. (2002, 2004), applying least squares technique and neural network, developed models using horizontal component of magnetic field from EEJ and drift velocity observations from Peruvian sectors. The magnetic field and drift velocity observations used for model development were taken from Peruvian sector. This model gives a prescription for the climatological characteristics of the plasma drift velocity anywhere along the equator even if the data for model development are obtained only from a single station (Peruvian longitudinal sector). Its performance showed a good agreement with Jicamarca radio observatory Incoherent Scatter Radar observations (Anderson et al., 2004), which is of course where the modeling data are taken from, and it should be evaluated for other longitudinal sectors. Its performance has been tested for the Peruvian and Philippines longitudinal sectors, and the result showed excellent and good agreement, respectively (Anderson et al., 2006). The root-mean-square error that can be incorporated in this model is about 3.5 m/s (Anderson et al., 2004).

The drift velocity and electric field models mentioned above have been developed without or with very few ground observations from the African and Asian regions. This implies that scarcity of data in these sectors has been a major problem in developing regional and global low-latitude ionospheric model until recently. At present, numbers of ionospheric monitoring instruments such as GPS receivers and ground-based magnetometers have been installed in the African sector (Amory-Mazaudier et al., 2009; Yizengaw & Moldwin, 2008), as well as in Asian sectors. In addition, Communication/Navigation Outage Forecasting System (C/NOFS) satellite, which was functional between 2008 and 2015, observed equatorial ionospheric parameters in all longitudes between $\pm 13^\circ$ latitudes. Vertical drift and ion density are examples of ionospheric parameters observed by this satellite. The new data available from these equatorial ionospheric monitoring devices are very important to validate and improve the performances of these models or develop new modeling technique. Having this resources, Habarulema et al. (2018) developed recently an empirical model to describe the climatological relationship between C/NOFS vertical ion plasma drift and ΔH observations but their work was restricted to one longitudinal sector Jicamarca (geographic; 11.8°S , 77.2°W). Dubazane and Habarulema (2018) also developed an empirical model of vertical ion drift for the African sector. The performance of this recently developed model has been tested over the African longitudinal sector and showed a good agreement.

EEJ is an intense current flowing eastward during the day bounded between the geomagnetic latitudes of 3°N and 3°S . The magnetic field due to this current can be modeled using Ampere's law (Brekke, 1997), which can be done by considering the EEJ as a set of parallel wires carrying currents in the east direction. Having the current density and induced magnetic field, the EEJ electric field can be inferred by using Ohm's law. Studies suggest that due to lack of sufficient data from every local region, physics-based calculations are better for modeling local phenomena than other empirical and climatological models (global-scale models; e.g., Yizengaw & Moldwin, 2008, and the references therein).

Therefore, in this paper a new technique of estimating vertical plasma drift velocity is introduced using parameterized and data-driven physics-based model with data obtained from ground-based magnetometer

Table 1
Geographic and Magnetic Coordinates of Magnetometers (Minus Sign Indicates Southern or/and Western Hemisphere)

Magnetometer stations	Code	Geog. latitude	Geog. longitude	Mag. latitude	Mag. longitude
JRO, Peru	JICA	-11.80	-77.20	0.80	-5.70
Petrolina, Brazil	PETR	-9.50	-40.50	-6.95	30.20
Abuja, Nigeria	ABJA	10.50	7.55	0.55	79.63
Cameroon, Cameroon	CMRN	3.87	11.52	-5.30	83.12
Addis Ababa, Ethiopia	AAE	9.00	38.80	0.90	110.50
Adigrat, Ethiopia	ETHI	14.28	39.46	5.90	111.06
Phuket, Thailand	PUKT	7.90	98.40	-0.60	169.95
Bangkok, Thailand	BANG	14.10	100.60	6.20	172.20

stations over different longitudinal sectors of the globe. The performance of the new technique and the existing two models are evaluated using drift velocity measurements from C/NOFS satellite.

2. Data and Modeling Techniques

2.1. Data

Data from pairs of magnetometers, over four longitudinal sectors (South America, West Africa, East Africa, and Asia) installed on (between 0° and $\pm 2^\circ$) and off magnetic equator (between $\pm 6^\circ$ and $\pm 9^\circ$), are taken for this study. Table 1 shows the magnetic and geographic locations of the stations. Available quiet day's data based on the Geosciences Australia (<http://www.ga.gov.au/>) during 2012 and 2015 have been used. Based on this criterion, we have obtained 24 days of data and all of them are used for modeling and analysis. Our model is validated using vertical drift observation from C/NOFS satellite. C/NOFS was an American satellite developed by the Air Force Research Laboratory Space Vehicles Directorate to investigate and

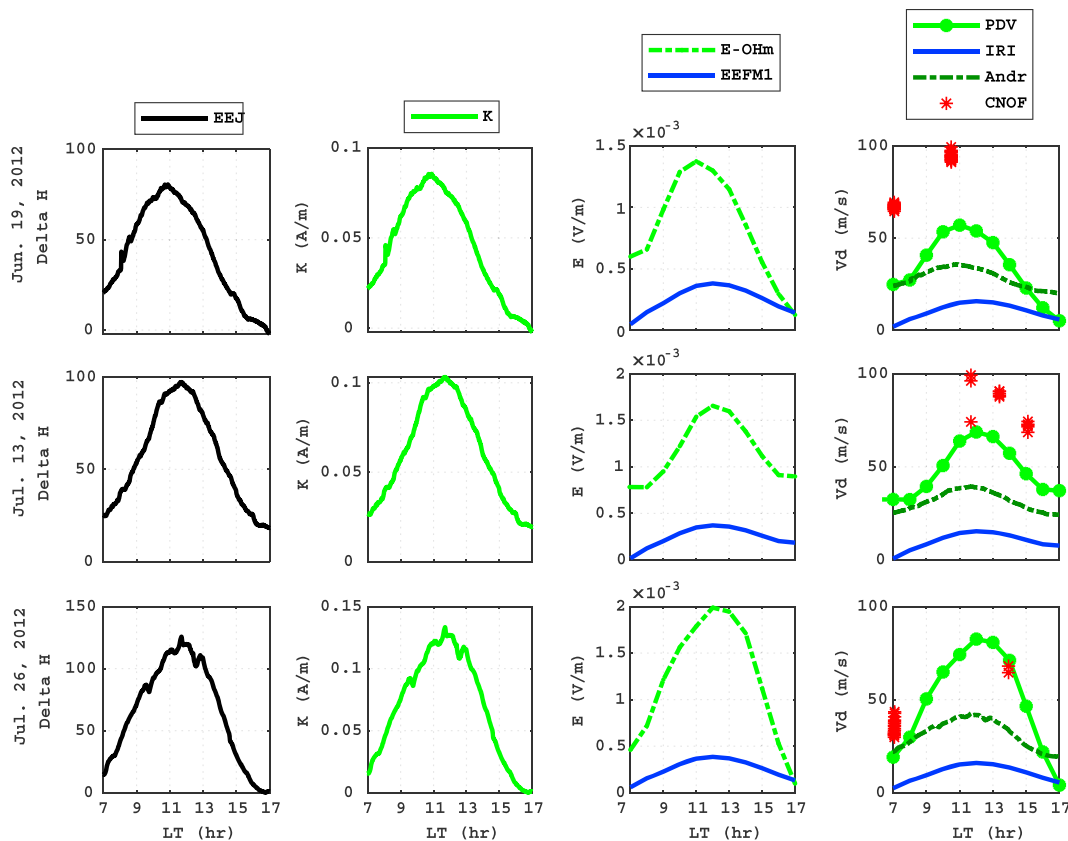


Figure 1. Daytime EEJ, estimated sheet current density, E field, and vertical ion drift over Jicamarca Radio Observatory, Peru, on 19 June and 13 and 26 July 2012.

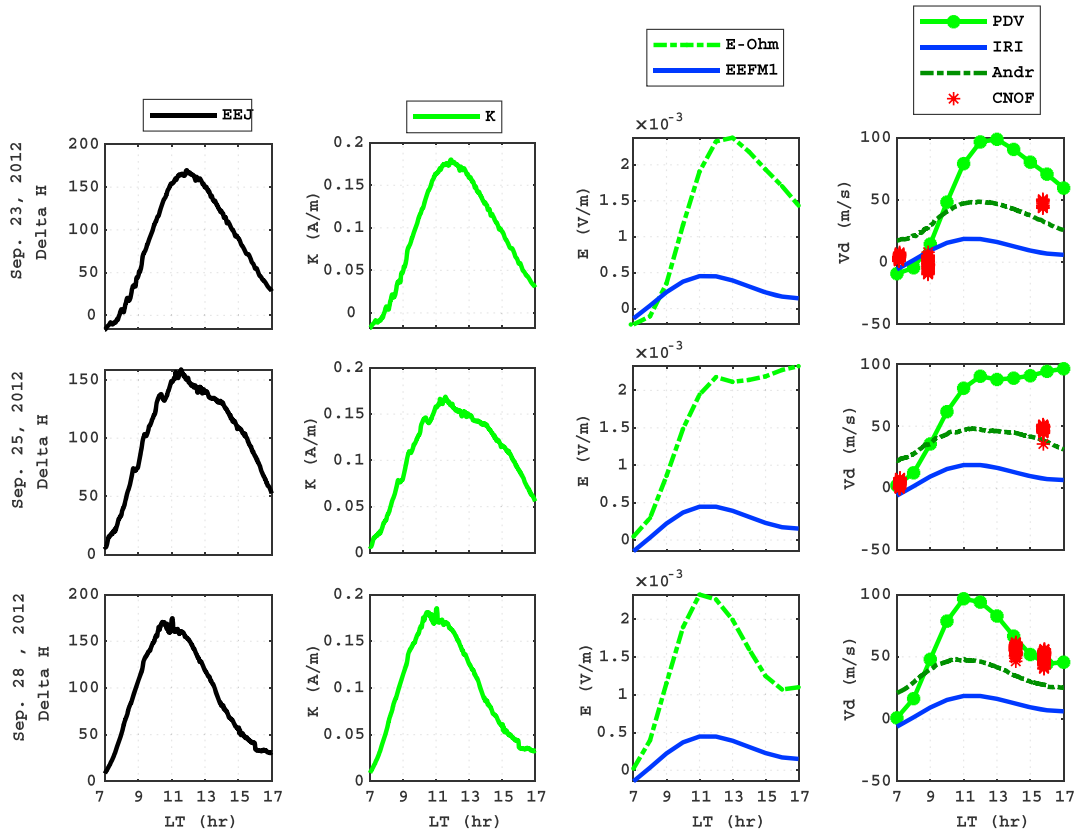


Figure 2. Daytime EEJ, sheet current density, E field, and vertical ion drift over Jicamarca Radio Observatory, Peru, on 11, 23, and 28 September 2012.

forecast scintillations and electrodynamics of in the Earth's equatorial ionosphere. Four payloads on board C/NOFS were operational to measure different ionospheric parameters such as ion density, ion temperature, vertical plasma drift velocity, and so on. The average uncertainty of vertical drift velocity measurement from C/NOFS is about 2.5 m/s. Detail about C/NOFS satellite and measuring techniques is found in Rodrigues et al. (2011). C/NOFS vertical drift data with tolerance distance (in degrees) not more than 3° of latitude and 5° of longitude from the on-equator station are taken for comparison.

2.2. Modeling Techniques

A magnetometer installed either on or off the magnetic equator on the surface of the Earth measures the net magnetic field due to space (EEJ and solar quiet currents) and ground sources (currents from Earth's core and mantle). Most often, EEJ enhances the horizontal component of geomagnetic field strength with in $\pm 5^\circ$ of the magnetic equator. Measuring the perturbation in the horizontal (H) component over the dip equator could provide a direct measure of the EEJ. The basic consideration is that the effect of the Sq currents in the dip equatorial region ground-based magnetometer is the same as that outside the extent of the EEJ, that is, $\pm 6^\circ - \pm 9^\circ$ off the dip equator (Anderson et al., 2004).

The nighttime baseline value, H_b , is the geomagnetic field strength, which is negligibly affected by external sources such as EEJ (Anderson et al., 2004). The baseline values were determined by taking the average of nighttime magnetic field strength. The magnetic fields due to sources in space are obtained by subtracting the baseline from each magnetic measurements of the magnetometer at the equator and off the equator given respectively by

$$\Delta H_{\text{equ}} = H_{\text{equ}} - H_{b(\text{equ})} \quad (1)$$

$$\Delta H_{\text{non-equ}} = H_{\text{non-equ}} - H_{b(\text{non-equ})} \quad (2)$$

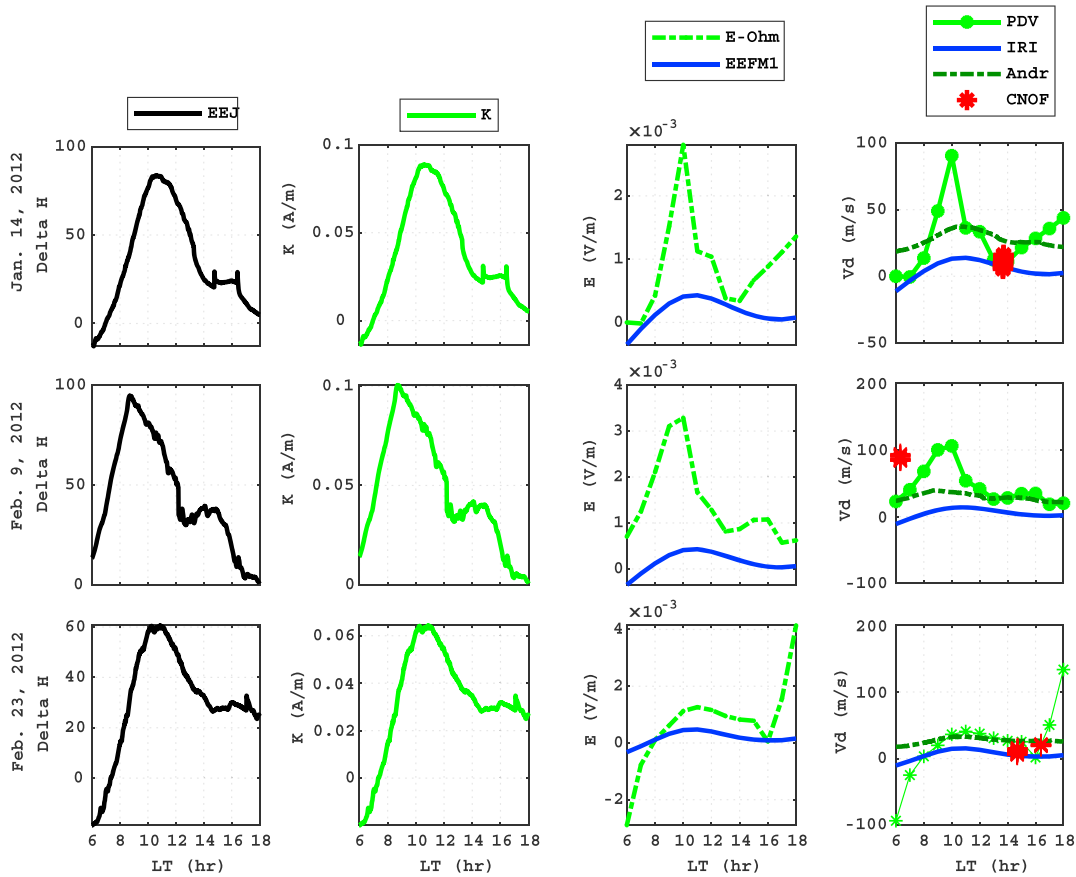


Figure 3. Daytime EEJ, sheet current density, E field, and vertical ion drift over Abuja, Nigeria, on 14 January, 9 and 23 February 2012.

where ΔH_{equ} and $\Delta H_{\text{non-equ}}$ stand for the total external magnetic field sources on and off the magnetic equator, respectively. $H_{b(\text{equ})}$ and $H_{b(\text{non-equ})}$ are nighttime baseline magnetic field measurements on and off the magnetic equator, respectively. B field from EEJ can be determined by removing the ring current and global Sq dynamo contribution to the H component of the magnetic field recorded by magnetometer at the magnetic equator. This is done by subtracting the total external magnetic field sources recorded off the magnetic equator ($\Delta H_{\text{non-equ}}$) from sources recorded on the magnetic equator (ΔH_{equ}) assuming that the effect of these currents at and off the equator ($\pm 6^\circ - \pm 9^\circ$) is approximately same. As clearly expressed in Brekke (1997), the magnetic field due to this current can be modeled using Ampere's law (i.e., considering the EEJ as a set of parallel wires carrying currents ($J = J_0$), the magnetic field outside can be determined using Ampere's loop) as

$$B = \frac{1}{2} \mu_0 J_0 b, \quad (3)$$

where $\mu_0 = 4\pi \times 10^{-7} \text{H/m}$ is permeability of free space and b is the current sheet thickness. Equation (3) indicates that the magnetic field outside the sheet is independent of the distance from the sheet. In the limit where the sheet is infinitesimally thin, $b \rightarrow 0$, instead of current density $J = J_0$, surface current, $K = K_x \hat{i}$, where $K_x = J_0 b$ with dimension A/m can be used (Brekke, 1997). Now for this study the EEJ magnetic field measurement model can be represented by

$$\Delta H = \frac{\mu_0 K_x}{2}, \quad (4)$$

where $B = \Delta H_{\text{equ}} - \Delta H_{\text{non-equ}}$. However, for a conducting Earth the factor $1/2$ must be substituted by $3/4$ (Brekke, 1997; Hargreaves, 1992). The EEJ current density and the east-west directed electric field can be related by

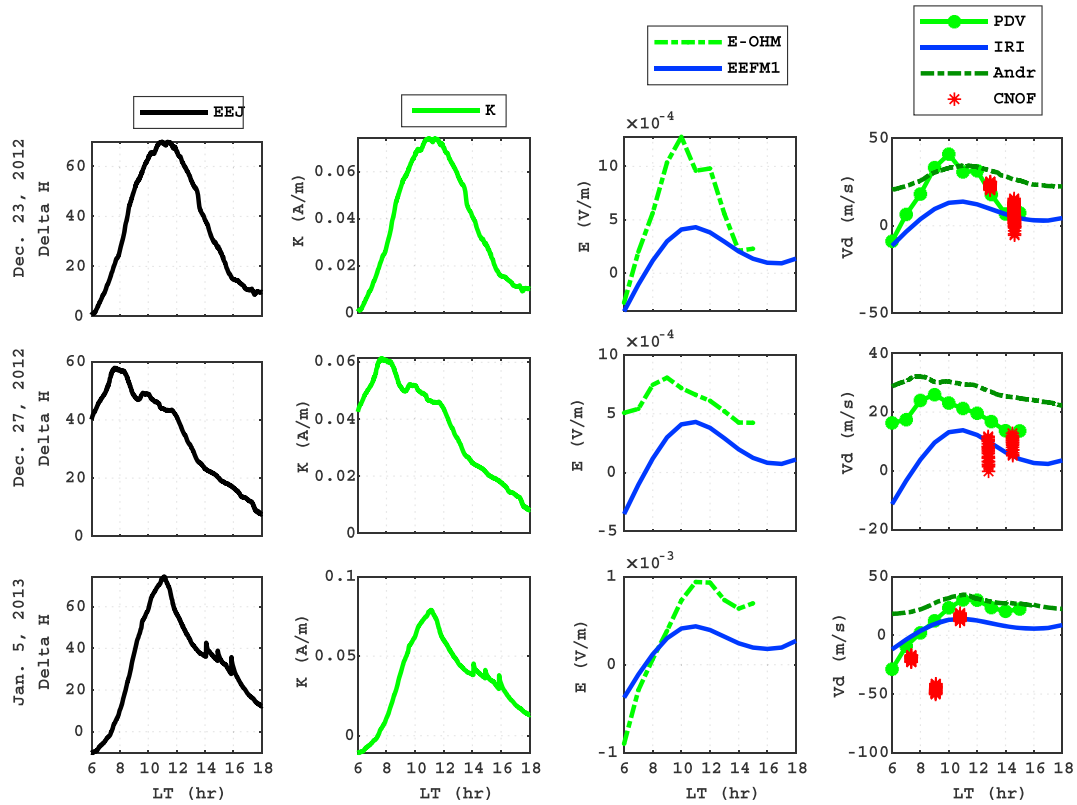


Figure 4. Daytime EEJ, sheet current density, E field, and vertical ion drift over Abuja, Nigeria, on 23 and 27 December and 5 January 2012.

$$K_x = \sum_C E, \quad (5)$$

where \sum_C is the height-integrated cowling conductivity and is given by Pfaff et al. (1997) as

$$\sum_C = \sum_P + \frac{\sum_H^2}{\sum_P} \quad (6)$$

where \sum_P and \sum_H are height-integrated Pederson and Hall conductivities, respectively. For this work the height-integrated Pederson and Hall conductivities are taken from Japanese world data center for geomagnetism (<http://swdc234.kugi.kyoto-u.ac.jp/ionocond/signal/index.html>). Thus, the east-west directed electric field can be determined by combining the above expressions. This electric field can be mapped to the F region along the equipotential geomagnetic field lines and produce the plasma drift velocity at an altitude h in the F region that is given by

$$V_d = \frac{\mathbf{E} \times \mathbf{B}(h)}{|\mathbf{B}(h)|^2}, \quad (7)$$

where $B(h)$ is the horizontal component of the Earth's magnetic field that can be determined at an altitude h in the F region. $B(h)$ has been estimated using the 12th Generation International Geomagnetic Reference Field (IGRF) model (<http://geomag.colorado.edu/igrf-mag-elements-calculator>). Generally, this equation is our parameterized model to estimate drift velocity using magnetometer measurements.

The east-west electric field has been compared also with equatorial electric field model (EEFM1) by Manoj et al. (2013). This model is obtained by inverting the magnetic signature of the EEJ for the current density. The model provides the climatological mean and variance of the EEJ as a function of longitude, local time, season, solar flux, and lunar local time (Alken & Maus, 2009; Manoj et al., 2013), where the climatological models are those simulating physical phenomena on a global scale and on a long time scale.

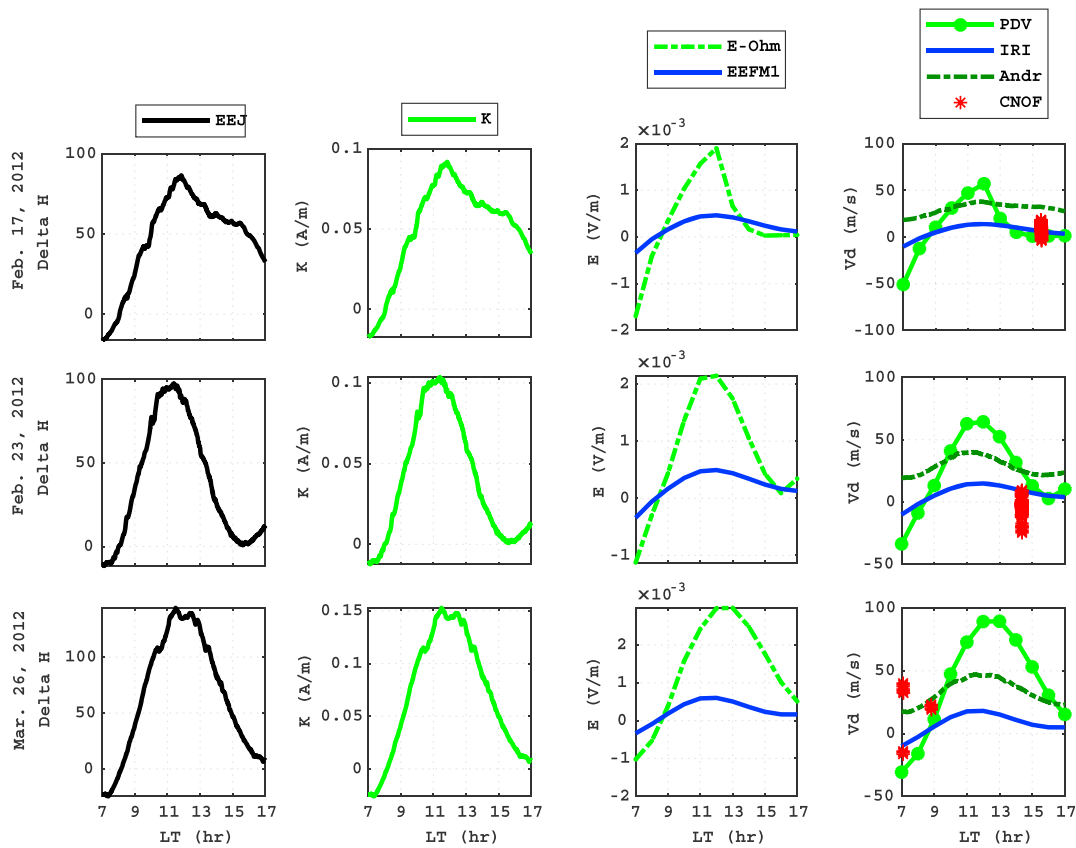


Figure 5. Daytime EEJ, sheet current density, E field, and vertical ion drift over Addis Ababa, Ethiopia, on 17 and 23 February and 26 March 2012.

One-minute average magnetic field measurements have been used as an input to the models used in this study such as our parameterized drift velocity (PDV) and Anderson models. The output of these models including that of the IRI-2016 vertical drift model, which is originally from Scherliess and Fejer (1999), is evaluated using the 1-min in situ observation of the drift velocity as obtained from the C/NOFS satellite ion velocity meter.

3. Results and Discussions

3.1. Diurnal Variations of Vertical Drift Velocities Over Four Longitudinal Sectors

Diurnal variations of EEJ (ΔH), E field, sheet current density (K), and vertical drift velocity are analyzed for four longitudinal sectors, and we have considered days from both equinoctial and solstices to see the seasonal performance of those models. In Figure 1, from the left, the first column shows the daytime ΔH variations over Peruvian sector on 19 June and 13 and 26 July 2012. The second column is the sheet current density at an altitude of about 110 km calculated from equation (4) and ΔH observation. The third column shows the E field estimated from EEFM1 E field model (Manoj et al., 2013; blue curve) and simplified model (i.e., equation (5)) based on Ohm's law (the broken green curve). The rightmost column depicts vertical drift velocities estimated using empirical models such as Anderson (represented by *Andr* on the figures) and the IRI-2016 (IRI on the figures) models and also using the simplified model based on Ohm's law (i.e., equation (7)) as a function of local time. The vertical drift velocity observations obtained from C/NOFS satellite are also shown in the same panel (red asterisks). The columns in Figures 2–8 below are similar to the panels explained for Figure 1.

As shown in Figure 1 (results obtained for the Peruvian sector), ΔH and K present daytime peaks at around 1200 LT on the 3 days. On the third column, the E field from Ohm's law shows a maximum discrepancy near

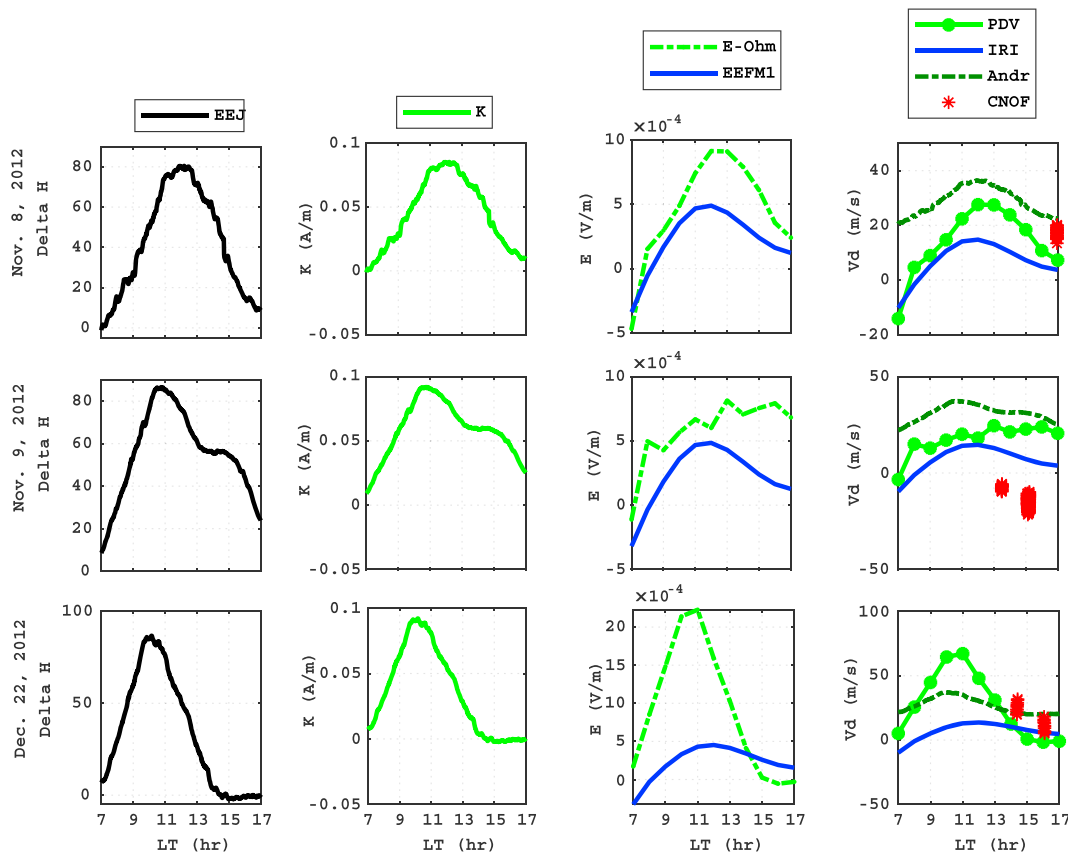


Figure 6. Daytime EEJ, sheet current density, E field, and vertical ion drift over Addis Ababa, Ethiopia, on 8 and 9 November and 22 December 2012.

to 1.5 mV/m from the EEFM1 model. As it is clearly seen, the diurnal patterns of drift velocity from all the three models are similar. However, there is clear magnitude variations. The drift velocities from Anderson model and Ohm's law have shown good agreement near sunrise and sunset, but they have also shown strong discrepancy around noontime. The drift velocity from IRI-2016 shows strong deviation from the other model results during almost all the sunlit hours. As can be seen in the plots, the model underestimated the drift velocities compared to the C/NOFS observations, marked by asterisks. In all of these 3 days the drift velocity observations have shown better agreement with our PDV model as compared to the outputs of other models. C/NOFS observations shown in this figure represented morning, noon, and afternoon hours. Similarly, Anderson's model performs better than IRI-2016 in all of the cases considered.

In the new technique of vertical ion drift estimation on the fourth column, a discrepancy of more than 20 m/s is seen from the other two models at around noontime and they agree at around postsunrise and presunset hours. But the prediction to the in situ observation is good when compared to these models in all the 3 days. On 13 and 26 July there is very good agreement of PDV model with the satellite data. As can be depicted from the 3 days, Anderson vertical drift model is comparably better than the IRI model.

Figure 2 shows results similar to Figure 1 but for equinoctial days of 11, 23, and 28 September 2012 to examine the performance of those models for the Peruvian region. The diurnal variations of ΔH , sheet current density, and E field have shown similar patterns. All of these quantities increase from morning to noontime and get maximum around noontime and then decreases. The E field estimated from EEFM1 model and the one from equation (7) have shown significant difference especially around noontime. Interestingly, the diurnal variations pattern of drift velocity estimated using equation (7) have shown similar pattern with the diurnal variations of ΔH , sheet current density, and E field. Except on 23 September in the afternoon, the drift velocities estimated from equation (7) have shown better agreement with C/NOFS observations as

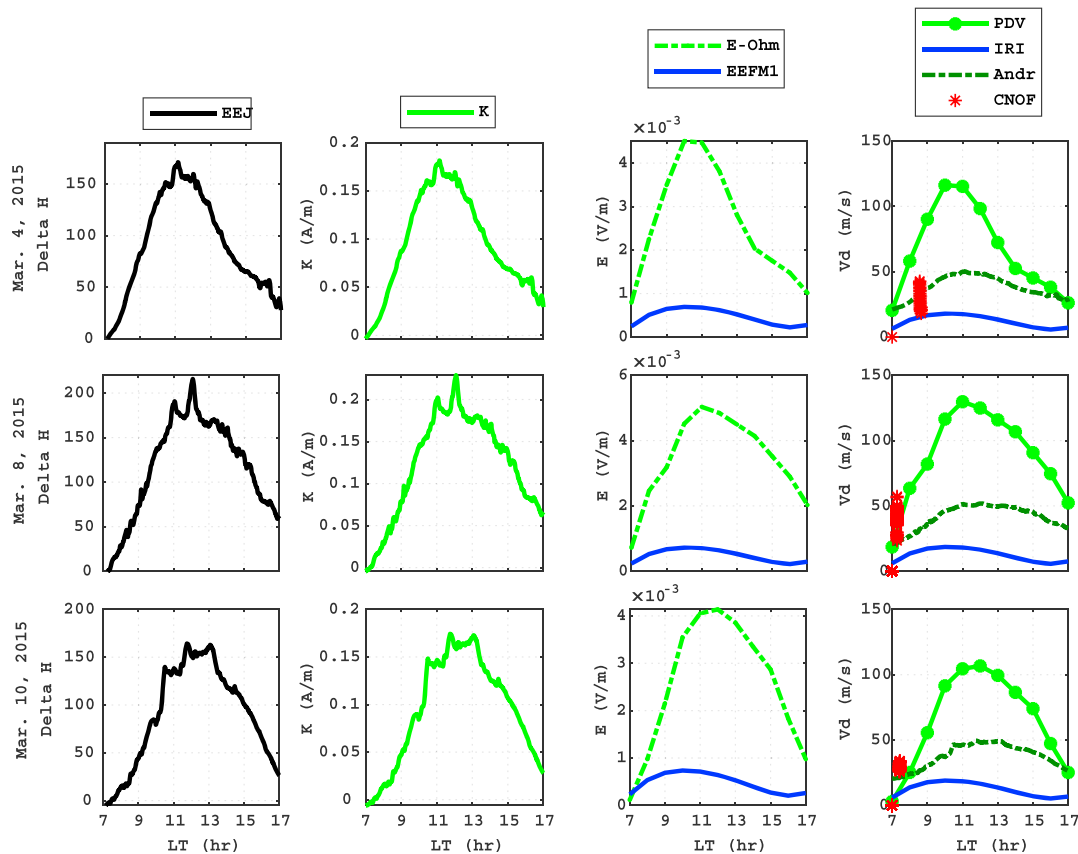


Figure 7. Daytime EEJ, sheet current density, E field, and vertical ion drift over Phuket, Thailand, on 4, 8, and 10 March 2015.

compared to the drift velocities estimated by the other models. The morning time downward vertical drifts and upward drift velocity observations at other time of the day are closely represented only by the new model proposed in this study (see panels for 23 September 2012). The peak values of ΔH and the corresponding E field shown in Figures 1 and 2 have shown clear difference. The peak values for these quantities respectively for Figure 1 are about 100 nT and 1.5 mV/m and for Figure 2 are above 150 nT and 2 mV/m. Similarly, vertical drift velocities for Figures 1 and 2 have shown differences. On 11 September PDV model and Anderson's model showed excellent performances and on 23 September, at about 0700- and 0900-LT PDV and IRI-2016 show better agreement with the C/NOFS observations. Again, on 28 September these two models agreed well to the measurement at 0700 LT, but on both 23 and 28 September the Anderson model shows good prediction than others. On 28 September, around 1400 and 1600 LT the PDV technique shows good estimation.

Figures 3 and 4 show results for Abuja, Nigeria, and West Africa similar to those shown for Jicamarca in Figures 1 and 2. As can be seen in these figures, sheet current density and E field and drift velocities obtained from physics-based models have shown similar diurnal patterns. From Figure 3, it can be seen that on 14 January 2012 both IRI-2016 and PDV models show good agreement to the C/NOFS observations and on 9 February, PDV and Anderson's models show better estimations. All the models show good performance on 23 February, but on a closer look it can be seen that the PDV technique estimates the C/NOFS observations most closely. Similarly, in Figure 4, on 23 December, the PDV technique estimates the available C/NOFS measurements better than others. On 27 December, IRI-2016 shows closest estimates than others but PDV model estimates are better than Anderson's model. On 5 January 2013, IRI-2016 and PDV models show good and comparable performances. All the models show good agreement to C/NOFS observations, and the discrepancies between the models are also less as compared to the assessed days in the Peruvian sector. Particularly, on 23 February 2012 and 5 January 2013, the agreement is excellent both among the models and also to the observations.

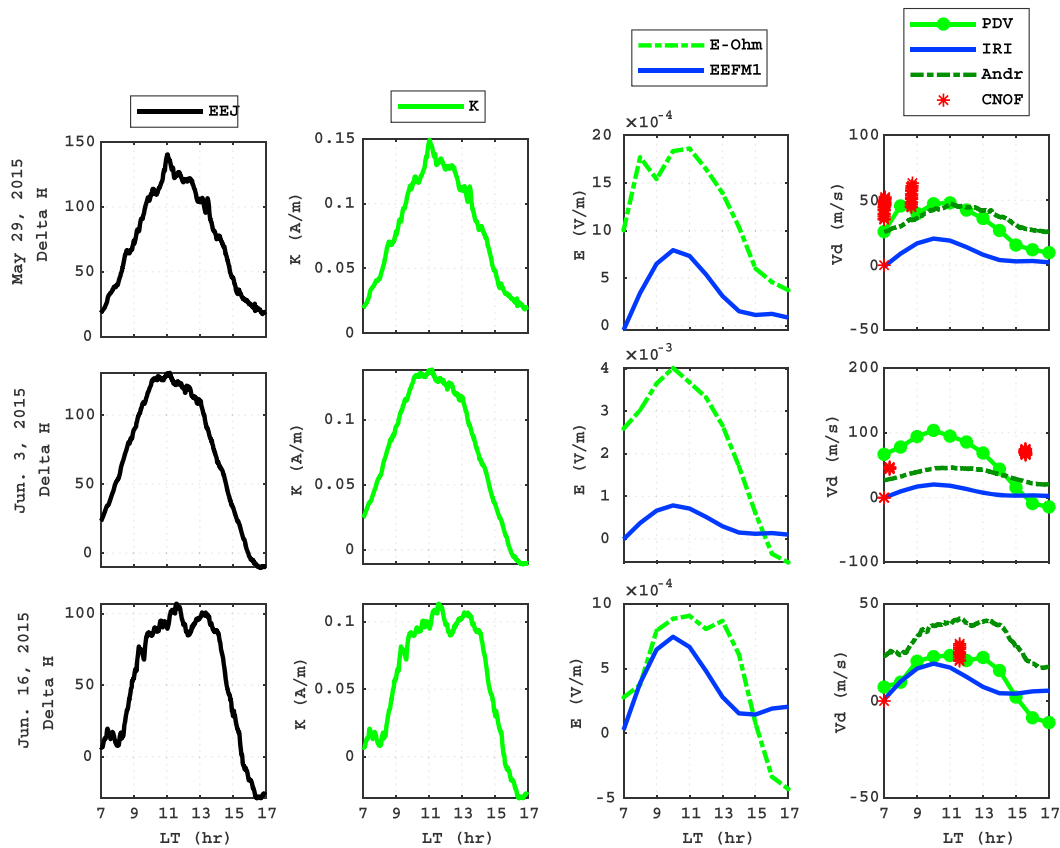


Figure 8. Daytime EEJ, sheet current density, E field, and vertical ion drift over Phuket, Thailand, on 29 May and 3 and 16 June 2015.

In Figures 5 and 6, we present similar analysis of the parameters we have seen in the Peruvian and West African sectors to the East African region. Compared to the days in Figure 6, days in Figure 5 show higher ΔH values (in magnitude), which might be a result of seasonal variations of the EEJ current. Gasperini and Forbes (2014) used magnetometer data from the Huancayo observatory in Peru, for the year 1990, and obtained results that indicate that 86% of the variance in the EEJ is due to the lunar-solar interaction. EEFM1 and Ohm's law-derived E field curves agree on the postsunrise and early sunset hours. On 17 February and 26 March 2012, the PDV drift velocity model agrees well with the C/NOFS measurements. On 8 November and 22 December 2012 (Figure 6) the observation is well estimated but there is a misfit on 9 November at about 1400 and 1600 LT where all the models show overestimations to the C/NOFS observations. This might have happened due to some local dynamical phenomena induced possibly by a propagating wave structure. Here, the IRI vertical drift model is closest to the measurement compared to the Anderson and PDV models.

Figures 7 and 8 are for the Asian longitudinal sector over Phuket, Thailand. The patterns are very similar to previous plots. Around noontime there exists large discrepancy between all the three models, but relatively, PDV technique and Anderson model show good agreement at the morning and evening hours. In contrast to the discrepancies seen between the models on the March equinox days, the PDV shows excellent match to other models and C/NOFS observations in Figure 8 featuring dates from summer solstice (29 May and 3 and 16 June 2015).

The C/NOFS measurement is available as in situ data source to clearly characterize the ionospheric dynamics and to evaluate the performance of different models like those mentioned above. From the diurnal variations of vertical drifts, we can verify that in most of the days considered, models which used ΔH (PDV and Anderson) as a basic input matched well with the satellite measurements for all sectors examined. It is indicated and described in Yizengaw et al. (2014) that a technique that uses magnetometer observations for vertical drift estimation has a tendency of better estimations or predictions. The ΔH values are found to be

high (magnitude) during the equinoctial days than those of the solstice. And this affects the result of the associated vertical ion drift estimates and shows high values as well, except on some cases where we believe that the model-derived cowling conductivity does not covariate with the sheet current density. Since we have taken a C/NOFS observation with spatial resolution tolerance of $\pm 3^\circ$ latitude and $\pm 5^\circ$ longitude, we believe that the PDV model discrepancies from the in situ observation on some instances arise from this approximations. In other words, the Cowling conductivity taken from world data center for geomagnetism at a specific location does not always correspond spatially to the C/NOFS measurements.

4. Conclusion

In this paper two well-known drift velocity models are validated against a new technique of estimating vertical plasma drift velocity using parameterized and data-driven physics-based (PDV) model. The new model uses magnetic field data obtained from different longitudinal regions. Electric field has been estimated using Ohm's law, and since it can map to the F region along the equipotential geomagnetic field lines, plasma drift velocity at an altitude h in the F region can then also be estimated using $\mathbf{E} \times \mathbf{B}/B^2$. The magnetic field due to an intense current flowing eastward during the day in the boundary between geomagnetic latitude of 3°N and 3°S is modeled using Ampere's law. In most of the cases presented (from Figures 1–8) the PDV model vertical drift velocity agreed well with the C/NOFS measurements except on few hours of some days compared to other models. We can conclude that the new technique employed in this paper gives promisingly good estimations for satellite observations. And this performance of our PDV model relies on its dependence on basic equations (equations (3) and (5)). Thus, assimilation to this technique can give a better and smoothed estimations.

Acknowledgments

The first author would like to thank Debre Tabor University and Air Force Materiel Command USAF fund, under Grant FA9550-16-1-0070, and the work of D. Hui is supported by the Department of Science and Technology, Government of India. We are also thankful for the different data sources (Samba-Amber magnetometers data center, Boston College), C/NOFS data (<https://spdf.gsfc.nasa.gov/pub/data/cnofs/cindi/>), and World magnetic data center, Kyoto University (<http://www.intermagnet.org/>).

References

- Alken, P., & Maus, S. (2009). Electric fields in the equatorial ionosphere derived from CHAMP satellite magnetic field measurements. *Journal of Atmospheric and Terrestrial Physics*, 72(4), 319–326. <https://doi.org/10.1016/j.jastp.2009.02.006>
- Amory-Mazaudier, C., Basu, S., Bock, O., Combrink, A., Groves, K., Fuller Rowell, T., et al. (2009). International Heliophysical Year: GPS Network in Africa. *Earth, Moon and Planets*, 104(1–4), 263–270. <https://doi.org/10.1007/s11038-008-9273-8>
- Anderson, D., Anghel, A., Chau, J., & Veliz, O. (2004). Daytime vertical $\mathbf{E} \times \mathbf{B}$ drift velocities inferred from ground-based magnetometer observations at low latitudes. *Space Weather*, 2, S11001. <https://doi.org/10.1029/2004SW000095>
- Anderson, D., Anghel, A., Chau, J. L., & Yumoto, K. (2006). Global, low-latitude, vertical $\mathbf{E} \times \mathbf{B}$ drift velocities inferred from daytime magnetometer observations. *Space Weather*, 4, S08003. <https://doi.org/10.1029/2005SW000193>
- Anderson, D., Anghel, A., Yumoto, K., Ishitsuka, M., & Kudeki, E. (2002). Estimating daytime vertical $\mathbf{E} \times \mathbf{B}$ drift velocities in the equatorial F-region using ground-based magnetometer observations. *Geophysical Research Letters*, 29(12), 1596. <https://doi.org/10.1029/2001GL014562>
- Brekke, A. (1997). *Physics of the upper polar atmosphere*. England: Praxis Publishing.
- Dubazane, M. B., & Habarulema, J. B. (2018). An empirical model of vertical plasma drift over the African sector. *Space Weather*, 16, 619–635. <https://doi.org/10.1029/2018SW001820>
- Farley, D. T., Bonelli, E., Fejer, B. G., & Larse, M. F. (1986). The prereversal enhancement of the zonal electric field in the equatorial ionosphere. *Journal of Geophysical Research*, 91(A12), 13723. <https://doi.org/10.1029/JA091iA12p13723>
- Fejer, B. G., & Kelley, M. C. (1980). Ionospheric irregularities. *Reviews of Geophysics and Space Physics*, 18(2), 401–454.
- Gasparini, F., & Forbes, J. M. (2014). Lunar-solar interactions in the equatorial electrojet. *Geophysical Research Letters*, 41, 3026–3031. <https://doi.org/10.1002/2014GL059294>
- Habarulema, J. B., Dubazane, M. B., Katamzi-Joseph, Z. T., Yizengaw, E., Moldwin, M. B., & Uwamahoro, J. C. (2018). Long-term estimation of diurnal vertical $\mathbf{E} \times \mathbf{B}$ drift velocities using C/NOFS and ground-based magnetometer observations. *Journal of Geophysical Research: Space Physics*, 123, 6996–7010. <https://doi.org/10.1029/2018JA025685>
- Haerendel, G., & Eccles, J. V. (1992). The role of the equatorial electrojet in the evening ionosphere. *Geophysical Research*, 97(A2), 1181–1192. <https://doi.org/10.1029/91JA02227>
- Hargreaves, J. K. (1992). *The solar-terrestrial environment*. Cambridge: the Press Syndicate of the University of Cambridge. <https://doi.org/10.1017/CBO9780511628924>
- Heelis, R. A. (2004). Electrodynamics in the low and middle latitude ionosphere: A tutorial. *Journal of Atmospheric and Terrestrial Physics*, 66(10), 825–838. <https://doi.org/10.1016/j.jastp.2004.01.034>
- Hui, D., & Fejer, B. G. (2015). Daytime plasma drifts in the equatorial lower ionosphere. *Journal of Geophysical Research: Space Physics*, 120, 9738–9747. <https://doi.org/10.1002/2015JA021838>
- Hysell, D. L., & Burcham, J. D. (2000). Ionospheric electric field estimates from radar observations of the equatorial electrojet. *Journal of Geophysical Research*, 105(A2), 2443–2460. <https://doi.org/10.1029/1999JA900461>
- Kelley, M. C., Ilma, R. R., & Crowley, G. (2009). On the origin of pre-reversal enhancement of the zonal equatorial electric field. *Annales de Geophysique*, 27(5), 2053–2056. <https://doi.org/10.5194/angeo-27-2053-2009>
- Kelley, M. C. (2009). *The Earth's ionosphere: Plasma physics and electrodynamics* (2nd ed.). Amsterdam, Boston: Elsevier.
- Manoj, C., Maus, S., & Alken, P. (2013). Long-period prompt-penetration electric fields derived from CHAMP satellite magnetic measurements. *Journal of Geophysical Research: Space Physics*, 118, 5919–5930. <https://doi.org/10.1002/jgra.50511>
- Pfaff, R. F. Jr., Acuna, M. H., Marioni, P. A., & Trivedi, N. B. (1997). DC polarization electric field, current density, and plasma density measurements in the daytime equatorial electrojet. *Geophysical Research Letters*, 24, 1667–1670.

- Rastogi, R. G., & Klobuchar, J. A. (1990). Ionospheric electron content within the equatorial F₂ layer anomaly belt. *Journal of Geophysical Research*, 95(A11), 19,045–19,052. <https://doi.org/10.1029/JA095iA11p19045>
- Rodrigues, F. S., Crowley, G., Azeem, S. M. I., & Heelis, R. A. (2011). C/NOFS observations of the equatorial ionospheric electric field response to the 2009 major sudden stratospheric warming event. *Journal of Geophysical Research*, 116, A09316. <https://doi.org/10.1029/2011JA016660>
- Scherliess, L., & Fejer, B. G. (1999). Radar and satellite global equatorial F-region vertical drift model. *Journal of Geophysical Research*, 104(A4), 6829–6842. <https://doi.org/10.1029/1999JA900025>
- Sreeja, V., Devasia, C. V., Ravindran, S., & Pant, T. K. (2009). Observational evidence for the plausible linkage of Equatorial Electrojet (EEJ) electric field variations with the post sunset F-region electrodynamics. *Annales de Geophysique*, 27, 4229–4238. <https://doi.org/10.5194/angeo-27-4229-2009>
- Sridharan, S., Sathishkumar, S., & Subramanian, G. (2009). Variabilities of mesospheric tides and equatorial electrojet strength during major stratospheric warming events. *Annales de Geophysique*, 27, 4125–4130. <https://doi.org/10.5194/angeo-27-4125-2009>
- Yizengaw, E., & Moldwin, M. B. (2008). African Meridian B-Field Education and Research (AMBER) array. *Earth, Moon and Planets*, 104(1-4), 237–246. <https://doi.org/10.1007/s11038-008-9287-2>
- Yizengaw, E., Moldwin, M. B., Zesta, E., Biouele, C. M., Damtie, B., Mebrahtu, A., et al. (2014). The longitudinal variability of equatorial electrojet and vertical drift velocity in the African and American sectors. *Annales de Geophysique*, 32(3), 231–238. <https://doi.org/10.5194/angeo-32-231-2014>